The Analysis of the Onset of Soret-Driven Convection in Nanoparticles Suspension

Min Chan Kim
Dept. of Chemical Engineering, Cheju National University, Cheju 690–756, Korea

Joung Sook Hong
ARC Center, Korea University, Seoul 136–701, Korea

Chang Kyun Choi
School of Chemical and Biological Engineering, Seoul National University, Seoul 151–744, Korea

DOI 10.1002/aic.10872
Published online April 19, 2006 in Wiley InterScience (www.interscience.wiley.com).

The onset of buoyancy-driven convection in an initially quiescent, horizontal nanoparticles suspension layer heated from above is analyzed theoretically. In this thermally-stable stratified fluid layer, the Soret diffusion can induce buoyancy-driven motion for the case of the negative separation ratio. For the high solutal Rayleigh number, the convective motion sets in during the transient diffusion stage and the onset time of this motion is analyzed by employing the propagation theory. Here the stability criteria are obtained and the predicted critical time to mark the onset of convective motion, τ_c, is compared with available experimental data. It is shown that convective motion can be detected starting from a certain time $\tau_m \cong 4\tau_c$. © 2006 American Institute of Chemical Engineers *AIChE J,* 52: 2333–2339, 2006

Keywords: nanoparticles suspension, buoyancy-driven convection, propagation theory, stability criteria, Soret effect

Introduction

Thermal convection in binary mixtures like ethanol-water and ^{3}He−^{4}He or various gas mixtures shows quite different characteristics from those in pure fluids.[1-4] Recently the onset of buoyancy-driven convection in nanoparticles suspension systems has attracted many researchers' interest.[5-9] If suspension of nanoparticles is under consideration, the spatiotemporal properties of convection in nanoparticles suspension are much more complex than those of pure fluids or molecular solutions due to the influence of thermal diffusion, that is, Soret-induced concentration gradients, and also the extremely small particle mobility that can be reflected by the Lewis number $Le \leq 10^{-4}$.

Correspondence concerning this article should be addressed to M. C. Kim at mckim@cheju.ac.kr.

Here $Le(= D_C/\alpha)$ is the Lewis number, D_C the diffusion coefficient, and α the thermal diffusivity. The separation ratio $\psi(= -\{\beta_C/\beta_T\}\{\nabla C/\nabla T\})$ is defined as the ratio between the density variations induced by solutal expansion and those induced by thermal expansion, where $\beta_T\ (= -\rho^{-1}(\partial\rho/\partial T))$ and $\beta_C\ (=\rho^{-1}(\partial\rho/\partial C))$ are the thermal and the solutal expansion coefficients, respectively. For Soret diffusion systems the separation ratio is usually defined as $\psi\ (=\{\beta_C/\beta_T\}\{D_T/D_C\})$, where D_T is the Soret diffusion coefficient and can be used as the measure of the relative importance of the Soret effect with respect to weak solutal diffusion.[5-9]. For the case of $\psi = 0$ double diffusive convection sets in when $Ra + Ra_s \geq 1708$,[10] where $Ra\ (=g\beta_T\Delta T d^3/\alpha\nu)$ is the thermal Rayleigh number and $Ra_s\ (= g\beta_C\Delta C d^3/D_C\nu)$ the solutal Rayleigh number, respectively.

For non-vanishing ψ, however, the external temperature gradient induces concentration variations and these create the

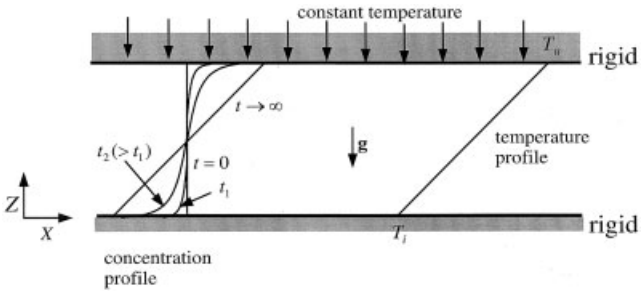

Figure 1. Basic system considered here.

buoyancy force. Depending on the sign of the separation ratio ψ, the solutal buoyancy force may act in the same direction as the thermal buoyancy force (for the case of positive ψ) but it counteracts to this force for the case of negative ψ. For the case of negative ψ, Soret effect can induce buoyancy-driven motion even in initially uniform concentration and thermally stable configurations. For the fully-developed linear temperature field, the critical Rayleigh number to represent the convective instability is $Ra_c = 720(Le/\psi)$ for the linear concentration field considering the relative time scale of mass diffusion with respect to thermal diffusion.[11]

In the present study the onset of Soret-driven convection in the horizontal fluid layer heated from above with large concentration difference, that is, $Ra(Le/\psi)^{-1} >> 720$, is investigated by using the propagation theory we developed.[12-14] This is a deterministic model using scaling relations and the momentary instability concept. In the propagation theory it is assumed that a most dangerous mode of disturbance will set in, experiencing instantaneous variations in their values upon their onset. The resulting stability criteria have compared well with experimental data for solidification,[15,16] Bénard-Rayleigh convection,[12,17,18] Marangoni-Bénard convection,[19,20] and Taylor-like vortices.[13,14,21] For the present problem the new stability equations will be derived based on the propagation theory. Our predictions will also be compared with available experimental results.[6,7,22]

Theoretical Analysis

The problem considered here is a horizontal fluid layer confined between two rigid plates separated by the vertical distance d. The basic system of pure conduction is shown in Figure 1. The fluid layer, of which Ψ has a large negative value, is initially quiescent at a constant concentration C_i and a constant temperature T_i. For time $t \geq 0$ the fluid layer is heated suddenly from above with a constant temperature T_u, that is, Ra has a negative value. For a high $Ra(Le/\psi)^{-1}$, buoyancy-driven convection will set in at a certain time and the governing equations of motion, temperature, and concentration fields are expressed by employing the Boussinesq approximation[23]:

$$\nabla \cdot \mathbf{U} = 0 \tag{1}$$

$$\left\{\frac{\partial}{\partial t} + \mathbf{U}\cdot\nabla\right\}\mathbf{U} = -\frac{1}{\rho_r}\nabla P + \nu\nabla^2\mathbf{U} + \mathbf{g}(\beta T - \beta_c C), \tag{2}$$

$$\left\{\frac{\partial}{\partial t} + \mathbf{U}\cdot\nabla\right\}T = \alpha\nabla^2 T, \tag{3}$$

$$\left\{\frac{\partial}{\partial t} + \mathbf{U}\cdot\nabla\right\}C = -\nabla\cdot\mathbf{j}, \tag{4}$$

$$\mathbf{j} = \mathbf{j}_D + \mathbf{j}_S = -D_C\nabla C - D_T\nabla T, \tag{5}$$

where U is the velocity vector, ρ the density, P the dynamic pressure, ν the kinematic viscosity, T the temperature, C the concentration, α the thermal diffusivity, g the gravitational acceleration, and β the expansion coefficient. The subscript r represents the reference state.

At the steady state the basic temperature and concentration profiles are linear and time-independent, and its critical condition is well summarized by Ryskin et al.[11] However, for the case of $Ra(Le/\psi)^{-1} >> 720$, convective motion can occur during the transient diffusion process, and the related stability problem becomes transient. Its critical time t_c to mark the onset of buoyancy-driven motion remains unsolved. For this transient stability analysis, we define a set of nondimensionalized variables τ, z, $\theta_0(=\{T_i - T\}/\Delta T)$ by using the scale of time d^2/D_C, length d, and temperature $\Delta T(=T_i - T_u)$. Then the basic conduction state is represented in dimensionless form of

$$\frac{\partial\theta_0}{\partial\tau} = \frac{1}{Le}\frac{\partial^2\theta_0}{\partial z^2}, \tag{6}$$

with the following initial and boundary conditions,

$$\theta_0(0, z) = \theta_0(\tau, 0) = \theta_0(\tau, 1) - 1 = 0. \tag{7}$$

The above equations can be solved by using the separation of variables:

$$\theta_0 = z + 2\sum_{n=1}^{\infty}\frac{(-1)^n}{n\pi}\sin(n\pi z)\exp\left(-\frac{n^2\pi^2}{Le}\tau\right). \tag{8}$$

For the case of nanoparticles suspension systems, the Lewis number is very small ($Le \approx 10^{-4}$) and, therefore, the basic temperature field can be approximated by

$$\theta_0 = z \quad \text{for } \tau \geq Le. \tag{9}$$

Based on the above temperature distribution, the dimensionless concentration field is given[23]:

$$\frac{\partial c_0}{\partial\tau} = \frac{\partial^2 c_0}{\partial z^2} \quad \text{for } \tau \geq Le, \tag{10}$$

under the following initial and boundary conditions,

$$c_0(0, z) = 0, \quad \frac{\partial c_0}{\partial z}(\tau, 0) = 1, \quad \frac{\partial c_0}{\partial z}(\tau, 1) = 1, \tag{11}$$

where $c_0 = Dc(C - C_i)/(j_s d)$ and $j_s = -D_T\Delta T/d$. For the case of negative ψ, the Soret flux j_s has a positive value. The boundary conditions have been obtained by the impermeable conditions for concentration at both boundaries, that is, $j = 0$

at $Z = 0$ and d. The above equations can be solved by using the separation of variables and also the Laplace transform:

$$\bar{c}_0(\tau, z) = z - \frac{1}{2} - \sum_{n=1}^{\infty} \frac{2((-1)^n - 1)}{(n\pi)^2} \cos(n\pi z)\exp(-n^2\pi^2\tau), \tag{12a}$$

$$c_0(\tau, \zeta) = \sqrt{4\tau} \sum_{\mathbf{n}=0}^{\infty} \left\{ -\text{ierfc}\left(\frac{n}{\sqrt{\tau}} + \frac{\zeta}{2}\right) - \text{ierfc}\left(\frac{n+1}{\sqrt{\tau}} - \frac{\zeta}{2}\right) + \text{ierfc}\left(\frac{n+1/2}{\sqrt{\tau}} - \frac{\zeta}{2}\right) + \text{ierfc}\left(\frac{n+1/2}{\sqrt{\tau}} + \frac{\zeta}{2}\right)\right\}, \tag{12b}$$

where $\zeta = z/\sqrt{\tau}$ and $\bar{c}_0 = c_0$. These solutions satisfy the mass conservation law of $(\partial/\partial\tau)(\int_0^1 c_0 dz) = 0$. The solution of c_0 in the (τ, ζ) coordinates converges more rapidly than that of $\bar{c}_0$ in the (τ, z) ones, especially for the case of small τ. For the deep-pool system of small τ ($Le \le \tau \le 0.01$) and ierfc $(\infty) = 0$, the basic concentration field is approximated by

$$c_0 = \sqrt{4\tau} \begin{cases} -\text{ierfc}\left(\dfrac{z}{2\sqrt{\tau}}\right) & \text{for } z \le 0.5, \\ \text{ierfc}\left(\dfrac{1-z}{2\sqrt{\tau}}\right) & \text{for } z \ge 0.5. \end{cases} \tag{13}$$

Here $-c_0(\tau, 0) = c_0(\tau, 1) = \sqrt{4\tau/\pi}$. The agreement with the exact solution is very good, as shown in Figure 2. With the above solutions, the following peculiar relation is shown:

$$\frac{\partial \bar{c}_0^*(\tau, z)}{\partial \tau} \approx -\frac{\zeta}{2\tau} \frac{\partial c_0^*(\tau, \zeta)}{\partial \zeta}, \tag{14}$$

where $(\bar{c}_0^*, c_0^*) = (\bar{c}_0, c_0)/\sqrt{\tau}$. The sign of equality is held for the limiting case of $\tau \to 0$. This means that from the chain rule of

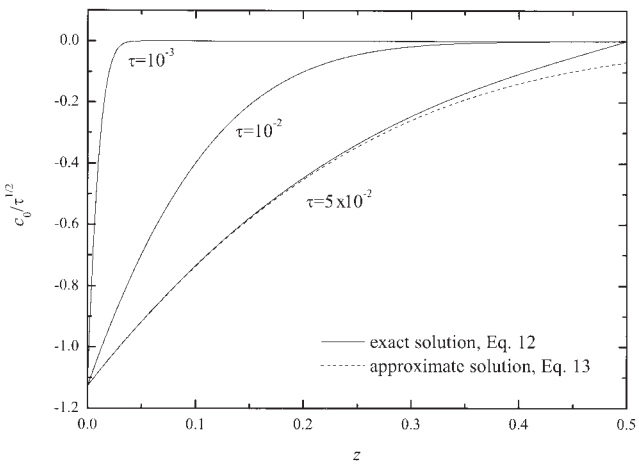

Figure 2. Comparison of basic concentration profiles.

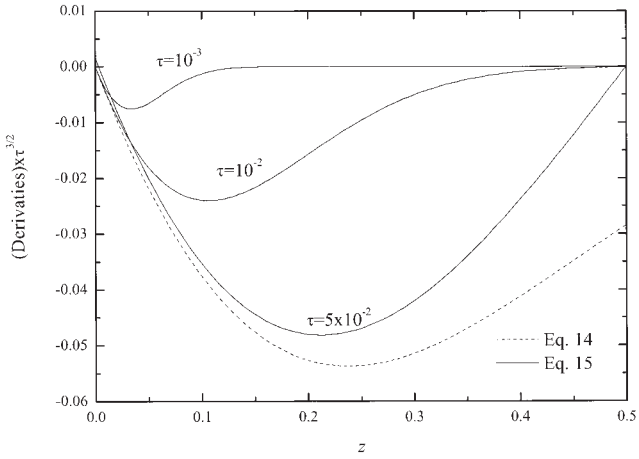

Figure 3. Comparison of Eq. 14 with Eq. 15 for the time derivative of the basic concentration.

$$\frac{\partial \bar{c}_0^*}{\partial \tau} = \frac{\partial c_0^*}{\partial \tau} + \frac{\partial c_0^*}{\partial \zeta}\frac{\partial \zeta}{\partial \tau} = \frac{\partial c_0^*}{\partial \tau} - \frac{\zeta}{2\tau}\frac{\partial c_0^*}{\partial \zeta}, \tag{15}$$

the first term in the right column is negligible with respect to the second term. In this case c_0^* becomes a function of ζ only and, therefore, ζ becomes a similarity variable like that in simple boundary-layer flows. Equation 14 agrees well with the exact one from Eq. 15 with decreasing time, as shown in Figure 3.

Over a certain time interval the concentration gradient, which is propagating from both boundaries, does not feel the presence of the other one, as shown in Figures 2 and 3. Based on this, Shliomis and Souhar[5] assumed the concentration gradient as

$$\frac{\partial c_0}{\partial z} = \text{erfc}\left(\frac{z}{2\sqrt{\tau}}\right), \tag{16}$$

and they further approximated it as

$$\frac{\partial c_0}{\partial z} = \begin{cases} 1 - z/\delta_s & \text{for } z \le \delta_s \\ 0 & \text{for } z > \delta_s, \end{cases} \tag{17}$$

where the diffusion skin layer $\delta_s = 4\sqrt{\tau/\pi}$ satisfies $\int_0^{\delta_s}(1 - z/\delta)dz = \int_0^{\infty} \text{erfc}[z/(2\sqrt{\tau})]dz$. By employing this concentration profile, they analyzed self-oscillatory convection caused by the Soret effect.

Stability Equations

Under linear stability theory, the nondimensionalized conservation equations incorporating the Soret effect are constituted as follows:

$$\left(\frac{1}{Sc}\frac{\partial}{\partial \tau} - \nabla^2\right)\nabla^2 w = \nabla_1^2 c_1 - \frac{1}{Le}\nabla_1^2\theta_1, \tag{18}$$

$$\frac{\partial c_1}{\partial \tau} + Rs\frac{\partial c_0}{\partial z}w = \nabla^2\left(c_1 + \frac{\Psi}{Le}\theta_1\right), \tag{19}$$

$$Le\left\{\frac{\partial\theta_1}{\partial\tau}+Raw\right\}=\nabla^2\theta_1, \tag{20}$$

under the following boundary conditions,

$$w_1=\frac{\partial w_1}{\partial z}=\frac{\partial c_1}{\partial z}=\theta_1=0 \quad \text{at } z=0 \quad \text{and} \quad z=1, \tag{21}$$

where w_1, c_1, and θ_1 represent dimensionless disturbance quantities of the vertical velocity, concentration, and temperature, respectively. Here $\nabla^2=(\partial^2/\partial x^2)+(\partial^2/\partial y^2)+(\partial^2/\partial z^2)$, $\nabla_1^2=(\partial^2/\partial x^2)+(\partial^2/\partial y^2)$, and Rs $(=Ra(\psi/Le))=(g\beta_C j_S d^4/D_C^2\nu)$.

For the limiting case of very small Lewis numbers, the temperature disturbance governed by Eqs. 20 and 21 has the solution of $\theta_1=0$. Therefore, the disturbance equations reduce to:

$$\left\{\frac{1}{Sc}\frac{\partial}{\partial\tau}-\nabla^2\right\}\nabla^2 w_1=\nabla_1^2 c_1, \tag{22}$$

$$\frac{\partial c_1}{\partial\tau}+Rsw_1\frac{\partial c_0}{\partial z}=\nabla^2 c_1, \tag{23}$$

with the following boundary conditions,

$$w_1=\frac{\partial w_1}{\partial z}=\frac{\partial c_1}{\partial z}=0 \quad \text{at } z=0 \quad \text{and} \quad z=1. \tag{24}$$

Propagation Theory

Our goal is to find the critical time τ_c to mark the onset of convection for a given RS and SC by using Eqs. 22-24. With the amplification theory, the proper initial conditions at $\tau=0$ are required. The amplification theory is quite popular but its amplification factor to represent manifest convection should be decided experimentally. However, the propagation theory described below is a rather simple, deterministic approach even though it involves the transient effect. The present study will employ the propagation theory for the stability analysis.

The propagation theory employed for finding the critical time τ_c is based on the assumption that for a deep-pool system of small τ, temperature disturbances at the marginal state of instability are propagated mainly within the concentration boundary layer thickness Δ_C. So it is assumed that at the onset of convective motion, the following scale analysis in terms of the solutal penetration depth $\Delta_C(\propto t^{1/2})$ is valid for perturbed quantities of Eqs. 2 and 4, respectively:

$$\frac{\partial W_1}{\partial t}\sim\mu\nabla^2 W_1\left(\sim\mu\frac{W_1}{\Delta_C^2}\right)\sim\rho_r g C_1, \quad W_1\sim\frac{g\beta_C\Delta_c^2}{\nu}C_1, \tag{25a}$$

$$\frac{\partial C_1}{\partial t}\sim W_1\frac{\partial C_0}{\partial Z}\sim D_C\nabla^2 C_1\left(\sim D_C\frac{C_1}{\Delta_C^2}\right). \tag{25b}$$

The first scaling represents the balance between viscous and buoyancy forces, and the second one comes from that between convective and diffusive mass fluxes. Since motion is very weak near the onset time of instability, inertia force terms and convective flux terms except $W_1(\partial C_0/\partial Z)$ are negligible. Now, based on the above relations, the following amplitude relation can be obtained:

$$\left|\frac{w_1}{c_1}\right|\sim\delta_C^2\sim\tau. \tag{26}$$

We assume dimensionless amplitude functions of disturbances as

$$[w_1(\tau,z),\, c_1(\tau,z)]=[\tau^{n+1}\bar{w}^*(\tau,z),\, \tau^n\bar{c}^*(\tau,z)], \tag{27}$$

which satisfy Eq. 26. For small critical time we set $\bar{w}^*(\tau,z)=w^*(\tau,\zeta)$ and $\bar{\theta}^*(\tau,z)=\theta^*(\tau,\zeta)$ like Eqs. 12a and 12b. Here $\bar{w}^*$ and $\bar{\theta}^*$ are disturbances in the (τ,z) coordinates, while w^* and θ^* are those in the (τ,ζ) ones. Now, it is assumed that $\partial\bar{w}^*/\partial\tau\approx-(\zeta/(2\tau))(\partial w^*/\partial\zeta)$ and $\partial\bar{c}^*/\partial\tau\approx-(\zeta/(2\tau))(\partial c^*/\partial\zeta)$, which means that the disturbance amplitudes follow the property of the basic field (see Eq. 14).

At this stage a criterion to determine the exponent n in Eq. 27 is necessary. The system is supposed to be unstable at the time when the growth rate of a fastest growing disturbance (r_1) is larger than the growth rate of the basic quantity (r_0). They are here given as the root-mean-squared quantities of concentration components:

$$r_0=\frac{1}{E_B}\frac{dE_B}{d\tau}, \quad r_1=\frac{1}{E_D}\frac{dE_D}{d\tau}, \tag{28a,b}$$

where the subscripts B and D denote the basic and the perturbed state, respectively. The dimensionless energy E is defined by following the usual energy method:

$$E(\tau)=\frac{1}{2}\langle\mathbf{u}\rangle^2+\frac{1}{2}ScRa_s\langle c\rangle^2, \tag{29}$$

where u denotes dimensionless velocity vector and $\langle\cdot\rangle=\sqrt{(\int_V(\cdot)^2dV)/V}$. Here V denotes the dimensionless volume considered, such as one pair of vortices. For the case of $Sc\to\infty$ the dimensionless energy of Eq. 26 reduces to

$$E_B(\tau)=\frac{1}{2}\langle c_0\rangle^2, \quad E_D(\tau)=\frac{1}{2}\langle c_1\rangle^2. \tag{30a,b}$$

The critical time to mark the onset of a fastest growing mode of instability is here defined as the characteristic time when

$$r_0=r_1 \quad \text{at } \tau=\tau_c. \tag{31}$$

The case of $n=1/2$ in Eq. 27 satisfies the stability Eq. 31, with which the single-mode instability sets in at the earliest time τ_c with its corresponding wavenumber a_c. By the above reasoning we set $w_1=\tau^{3/2}w^*$ and $c_1=\tau^{1/2}c^*$. Now, the stability equations are obtained in dimensionless form from Eqs. 10 and 11 and then τ is fixed as τ_c. For large Sc, the resulting self-similar stability equations with $n=1/2$ are

$$(D^2 - a^{*2})^2 w^* = a^{*2} c^*, \tag{32}$$

$$\left(D^2 + \frac{1}{2}\zeta D - a^{*2} + \frac{1}{2}\right) c^* = Rs^* w^* Dc_0^*, \tag{33}$$

with the following boundary conditions,

$$w^* = Dw^* = Dc^* = 0 \quad \text{at } \zeta = 0 \quad \text{and as } \zeta \to \infty, \tag{34}$$

where $D = d/d\zeta$, $Rs^* = \tau_c^2 Rs^2$, and $a^* = a\sqrt{\tau_c}$.

For $\tau_c \geq 0.01$, Eqs. 32 and 33 are kept and Eq. 12 is used. In Eq. 34 the upper boundary $\zeta \to \infty$ is replaced with $z = 1$, that is, $\zeta = 1/\tau_c^{1/2}$, and in Eqs. 32 and 33 Rs^* and a^* are replaced with $Rs\tau_c^2$ and $a\tau_c^{1/2}$. Also, in Eq. 12, τ is replaced with τ_c but ζ is maintained. Since τ_c is the fixed parameter, the resulting stability equations are a function of ζ only. For a given Sc and τ_c, the minimum Rs_c value and its corresponding wavenumber a_c are obtained. For large time, the frozen-time model may be used under the assumption of $r_0 = r_1 = 0$ and the resulting stability equations reduce to $(D^2 - a^{*2})^2 w^* = a^{*2} c^*$ and $(D^2 - a^{*2}) c^* = Rs^* w^* Dc_0^*$.

Solution Method

The stability Eqs. 32-34 were solved by employing the outward shooting scheme. In order to integrate them, a trial value of the eigenvalue Rs^* and the boundary conditions $D^3 w^*$ and c^* at $\zeta = 0$ are assumed properly for a given a^*. Since the boundary conditions 34 are all homogeneous, the value of $D^2 w^*$ at $\zeta = 0$ can be assigned arbitrarily. This procedure is based on the outward shooting method in which the boundary value problem is transformed into the initial value problem. The trial values, together with the four known conditions at the heated boundary, give all the information to make numerical integration smoothly.

The integration based on the 4th-order Runge-Kutta method is performed from $\zeta = 0$ to a fictitious vertical distance to satisfy the infinite boundary conditions. By using the Newton-Raphson iteration, the trial values of Rs^*, $D^3 w^*$, and c^* are corrected until the stability equations satisfy the infinite boundary conditions within the relative tolerance of 10^{-10}. Then, by increasing the distance step by step, the above integration is repeated. Finally, the value of Rs^* is decided through the extrapolation. For the frozen-time model, the solution procedure is almost the same as above.

Results and Discussion

It is well-known that for large τ, the long wave instability of $a = 0$ is the preferred mode and the critical condition is $Rs_c = 720$.[11] For small τ the present neutral stability curve is given in Figure 4a. This yields the critical conditions:

$$\tau_c = 5.57 Rs^{-1/2}, \quad a_c = 0.2585 Rs^{1/4} \quad \text{as } \tau \to 0, \tag{33}$$

At this critical condition, the profiles of amplitude functions are featured in Figure 4b. From distributions of the basic concentration field (see Eq. 13) and the perturbation quantities, we obtain the following relation:

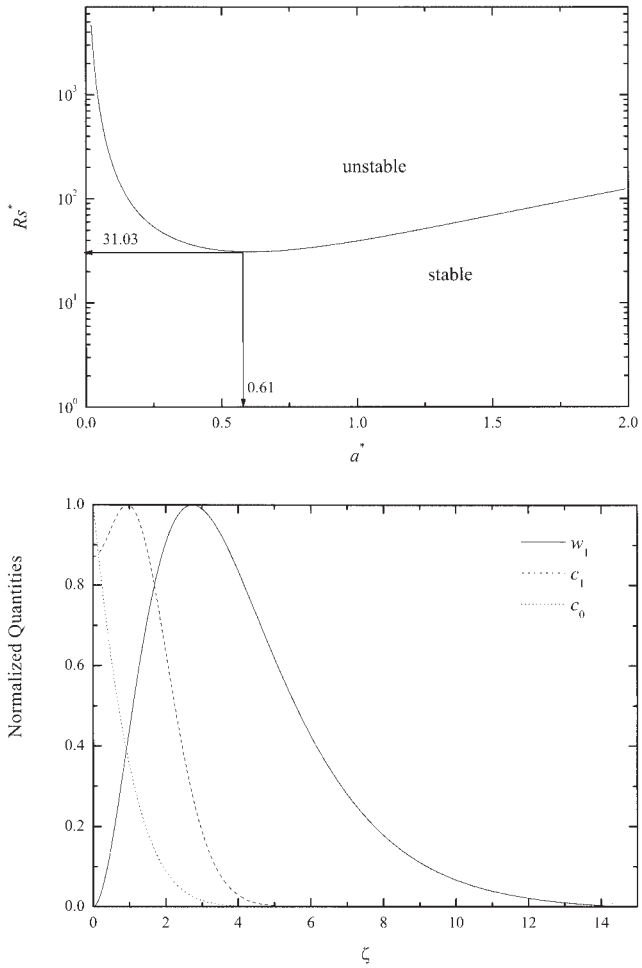

Figure 4. Stability conditions: (a) marginal stability curve and (b) distributions of amplitude functions.

$$r_0 = r_1 = \frac{3}{2\tau} \quad \text{as } \tau \to 0, \tag{34}$$

which satisfies the condition of the marginal state of instabilities we suggested, that is, Eq. 31. It is known that concentration disturbances are confined mainly within the solutal boundary layer and τ_c decreases with an increase in Rs. Equation 33 can be rewritten as a function of Ra_s:

$$\tau_c = 10.70 Ra_s^{-2/3} \quad \text{as } \tau \to 0, \tag{35}$$

since $Rs = Ra_s\sqrt{\pi/4\tau}$. This equation is less convenient in predicting τ_c but it is more useful for comparison with the system of $\Delta C =$ constant. Cerbino et al.[8] suggested a similar relation of $\delta^{-1} \sim (Rs\delta)^{0.35}$ where $\delta = \sqrt{\pi\tau^*}$. Their relation can be reformulated as $\tau^* \sim Ra_s^{-0.70}$, where τ^* is the latency time illustrated later. Their exponent -0.70 is quite similar to the present one: $-2/3$.

Foster[24] commented that $\tau_m \cong 4\tau_c$ with correct dimensional relations. Here τ_m is the onset time of manifest convection. This means that a fastest growing mode of instabilities, which sets in at $t = t_c$, will grow with time until manifest convection is detected at $t_m \cong 4t_c$ near the whole bottom boundary. A

growth period will be required, as illustrated in Figure 5. The validity of $t_m \cong 4t_c$ requires a further study, but this relation is kept even in other transient diffusive systems.[18,21] From Foster's viewpoint ($\tau_m \cong 4\tau_c$) the following relation is obtained:

$$\tau_m \approx 4\tau_c = 42.80 Ra_s^{-2/3} \quad \text{for } Rs \geq 10^6, \tag{36}$$

based on Eq. 34. Since the concentration difference increases continuously during the growth period ($\tau_c \leq \tau \leq \tau_m$), τ_m may be expressed as a function of Rs:

$$\tau_m = 42.80(Rs\sqrt{4\tau_m/\pi})^{-2/3} \quad \text{for } Rs \geq 10^6. \tag{37}$$

By using the shadowgraph method, Cerbino et al.[6,7] and Mazzoni et al.[22] visualized the Soret-driven convective motion in a suspension of 22 nm diameter silica particles (LUDOX®) dispersed in water. For this system $Le = 1.48 \times 10^{-4}$, $\psi = -3.41$, and $Sc = 3.7 \times 10^4$. They obtained the latency time τ^* and the peak time τ_p as the characteristic times when the variance of the intensity of images starts to grow and it shows the maximum value, respectively. They also measured the oscillation period τ_{osc} as a function of Rs. These experimental data are compared in Figure 5. As shown in this figure, our τ_m values bound the experimental τ^* values quite well. As expected, the peak time τ_p is a little larger than the latency time τ^*. It is interesting that our τ_m values are also close to the oscillation period τ_{osc}.

The present stability criteria are given:

$$Rs_c = 720, \quad a_c = 0 \quad \text{for } \tau \to \infty \tag{38}$$

which agree very well with those from the frozen-time model, as shown in Figure 5. The latter model is useful only for large time. The present critical wavenumber is featured in Figure 6. For large τ, a long wave instability is the preferred mode and the disturbances exist in the whole fluid layer.

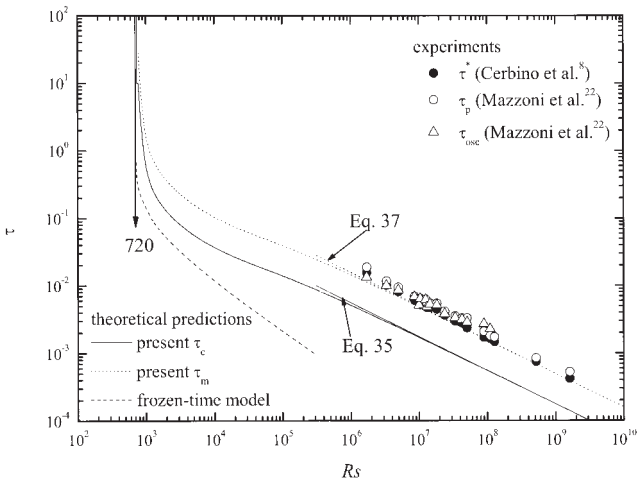

Figure 5. Comparison of critical times numbers with available experimental data.

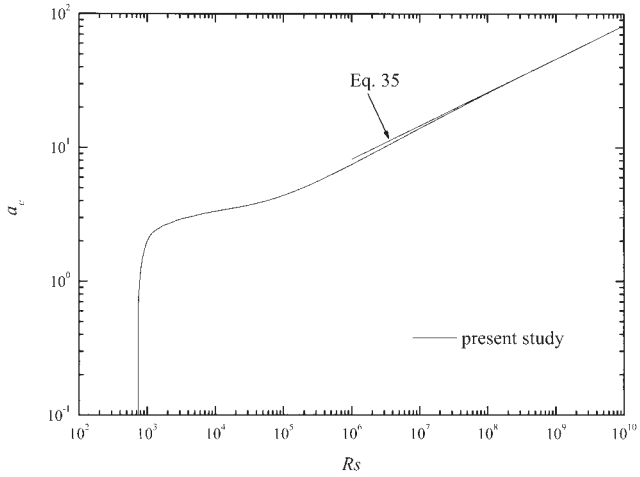

Figure 6. Predicted critical wavenumber.

Conclusions

The critical condition to mark the onset of convective motion driven by Soret diffusion in an initially quiescent, horizontal nanoparticles suspension layer heated from above has been analyzed by using the propagation theory. It seems that for deep-pool systems, manifest convection is detected at $\tau_m \cong 4\tau_c$ in comparison with available experimental data and for $\tau \leq \tau_m$, velocity disturbances are too weak to be observable experimentally. For small time the critical wavelength becomes smaller with increasing Rs while for large time a long wave mode ($a_c \to 0$) is the most unstable mode. The present results show that the propagation theory can be applied to the stability analysis of complex nanoparticles suspension systems without loss of generality.

Acknowledgments

This work was supported by the Korea Research Foundation Grant funded by the Korean Government (MOEHRD) (KRF-2005–041-D00182).

Literature Cited

1. Ahlers G, Rehberg I. Convection in a binary mixture heated from below. *Phys Rev Lett.* 1986;56:1373-1376.
2. Moses E, Steinberg V. Competing patterns in a convective binary mixture. *Phys Rev Lett.* 1986;57:2018-2021.
3. Liu J, Ahlers G. Rayleigh-Benard convection in binary-gas mixtures: thermophysical properties and the onset of convection. *Phys Rev E.* 1997;55:6950-6968.
4. La Porta A, Surko CM. Convective instability in a fluid mixture heated from above. *Phys Rev Lett.* 1998;80:3759-3761.
5. Shliomis MI, Souhar M. Self-oscillatory convection caused by the Soret effect. *Europhys Lett.* 2000;49:55-61.
6. Cerbino R, Vailati A, Giglio M. Soret driven convection in a colloidal solution heated from above at very large solutal Rayleigh number. *Phys Rev E.* 2002;66:055301(R).
7. Cerbino R, Vailati A, Giglio M. Fast-onset Soret-driven convection in a colloidal suspension heated from above. *Philos Mag.* 2003;83:2023-2031.
8. Cerbino R, Vailati A, Giglio M. Scaling behavior for the onset of convection in a colloidal suspension. *Phys Rev Lett.* 2005;94:064501.
9. Ryskin A, Pleiner H. Thermal convection in colloidal suspensions with negative separation ratio. *Phys Rev E.* 2005;71:056303.
10. Turner JS. *Buoyancy Effects in Fluids*. Cambridge University Press; 1973.
11. Ryskin A, Muller HW, Pleiner H. Thermal convection in binary

mixtures with a weak concentration diffusivity, but strong solutal buoyancy forces. *Phys Rev E.* 2003;67:046302.
12. Choi CK, Park JH, Kim MC, Lee JD, Kim JJ, Davis EJ. The onset of convective instability in a horizontal fluid layer subjected to a constant heat flux from below. *Int J Heat Mass Transfer.* 2004;47:4377-4384.
13. Kim MC, Choi CK. The onset of instability in the flow induced by an impulsively started rotating cylinder. *Chem Eng Sci.* 2005;60:599-608.
14. Kim MC, Chung TJ, Choi CK. The onset of Taylor-like vortices in the flow induced by an impulsively started rotating cylinder. *Theoret Comput Fluid Dynamics.* 2004;18:105-114.
15. Hwang IG, Choi CK. The onset of mushy-layer-mode instability during solidification in ammonium chloride solution. *J Crystal Growth.* 2000;220:326-335.
16. Hwang IG, Choi CK. Onset of compositional convection during solidification of a two-component melt from a bottom boundary. *J Crystal Growth.* 2004;267:714-723.
17. Yang DJ, Choi CK. The onset of thermal convection in a horizontal fluid layer heated from below with time-dependent heat flux. *Phys Fluids.* 2002;14:93-937.
18. Kim MC, Park JH, Choi CK. Onset of buoyancy-driven convection in the horizontal fluid layer subjected to ramp heating from below. *Chem Eng Sci.* 2005;60:5363-5371.
19. Kang KH, Choi CK. A theoretical analysis of the onset of surface-tension-driven convection in a horizontal liquid layer cooled suddenly from above. *Phys Fluids.* 1997;9:7-15.
20. Kang KH, Choi CK, Hwang IG. Onset of Marangoni convection in a suddenly desorbing liquid layer. *AIChE J.* 2000;46:15-23.
21. Kim MC, Choi CK. The onset of Taylor–Görtler vortices in impulsively decelerating swirl flow. *Korean J Chem Eng.* 2004;21:767-772.
22. Mazzoni S, Cerbino R, Vailati A, Giglio M. Transient oscillations in Soret-driven convection in a colloidal suspension. *Eur Phys J E.* 2004;15:305−309.
23. Hollinger St, Lucke M, Muller HW. Model for convection in binary liquids. *Phys Rev E.* 1998;57:4250−4264.
24. Foster TD. Onset of manifest convection in a layer of fluid with a time-dependent surface temperature. *Phys Fluids.* 1969;12:2482−2487.

Manuscript received Aug. 11, 2005, and revision received Mar. 8, 2006.